Available online at www.sciencedirect.com
SCIENCE DIRECT
Journal of Sound and Vibration 294 (2006) 615–623
JOURNAL OF SOUND AND VIBRATION
www.elsevier.com/locate/jsvi

Short Communication

Uncertainty quantification of an inflatable/rigidizable torus

Jiann-Shiun Lew[a,*], Lucas G. Horta[b], Mercedes C. Reaves[b]

[a]*Tennessee State University, Nashville, TN 37209, USA*
[b]*NASA Langley Research Center, Hampton, VA 23681, USA*

Received 3 October 2005; received in revised form 31 October 2005; accepted 27 November 2005
Available online 13 February 2006

Abstract

There is an increasing interest in lightweight inflatable structures for space missions. The dynamic testing and model updating of these types of structures present many challenges in terms of model uncertainty and structural nonlinearity. This paper presents an experimental study of uncertainty quantification of a 3m-diameter inflatable torus. Model uncertainty can be thought of as coming from two different sources, uncertainty due to changes in controlled conditions, such as temperature and input force level, and uncertainty associated with others random factors, such as measurement noise, etc. To precisely investigate and quantify model uncertainty from different sources, experiments, using sine-sweep excitation in the specified narrow frequency bands, are conducted to collect frequency response function (FRF) under various test conditions. To model the variation of the identified parameters, a singular value decomposition technique is applied to extract the principal components of the parameter change.

1. Introduction

There is an increasing interest in large ultra-lightweight space structures for space exploration with application to solar sails, large solar arrays, large aperture telescopes, and communication antennas [1–3]. Recently, a 3 m-diameter hexapod membrane structure was designed and built to conduct research on modeling and vibration control of this type of system [3]. Dynamic testing and modeling of this hexapod structure presents many challenges in terms of high modal densities, model uncertainty, and structural nonlinearities [4].

This paper presents an experimental investigation of uncertainty quantification of the torus of this hexapod structure. The previous study shows that the identified natural frequencies of the hexapod structure decreases as the input excitation increases [4]. In this paper, we will investigate and quantify the identified parameter uncertainty due to temperature variation and input force change. To generate high-quality data for the investigation of structural dynamics and the associated uncertainty, experiments with various levels of a sine-sweep signal in the specified narrow frequency ranges are conducted to measure frequency response function (FRF) data. In each specified narrow frequency band, many sets of FRF data are collected under various test

*Corresponding author. Tel.: +1 615 277 1607; fax: +1 615 277 1614.
E-mail address: lew@coe.tsuniv.edu (J.-S. Lew).

0022-460X/$ - see front matter © 2006 Elsevier Ltd. All rights reserved.
doi:10.1016/j.jsv.2005.11.029

conditions, different temperature ranges and various levels of input force. Following the FRF estimation, data are curve fitted with a least-squares technique to obtain the identified parameters [4,5].

Parametric uncertainty quantification has received considerable attention in the areas of model updating and validation [6,7]. Uncertainty quantification from experimental data plays a key role in model validation. The experimental outcome is used to compare and update the mathematical model from finite element analysis. Various approaches for the quantification of model uncertainty have been proposed recently [6,7]. Parametric uncertainties contributing to model uncertainty can be thought of as coming from two different sources. The first source of uncertainty is that due to changes in controlled conditions, such as temperature and input force level. A second source is the uncertainty associated with all others unconsidered factors, such as measurement noise, etc. In this paper, the controlled variables are temperature and the input force gain. A singular value decomposition (SVD) technique [4,8] is used to investigate and quantify the parametric uncertainty of the identified modal parameters in terms of natural frequencies and damping ratios.

2. Model uncertainty quantification

In this section, we will give a brief introduction of the uncertainty quantification approach [4]. The transfer function of a single input and single output system with displacement measurement can be written as

$$f(s) = \sum_{i=1}^{n} \frac{c_i}{s^2 + 2\xi_i\omega_i s + \omega_i^2}, \tag{1}$$

where ζ_i and ω_i are the damping ratio and natural frequency of the ith structural mode. The parameter vector of the identified natural frequencies and damping ratios can be defined as

$$\theta = \begin{bmatrix} \omega_1 & \xi_1 & \cdots & \omega_n & \xi_n \end{bmatrix}^{\mathrm{T}}. \tag{2}$$

Quantification of the parametric uncertainty is discussed in the following for some of the identified parameters. Experiments are conducted to identify models under various test conditions. The jth identified parameter vector for uncertainty quantification is defined as

$$p_j = \begin{bmatrix} p_{1j} & p_{2j} & \cdots & p_{kj} \end{bmatrix}^{\mathrm{T}}, \quad j = 1, 2, \ldots, m \tag{3}$$

where p_{ij} is the ith identified parameter, which can be damping ratio or natural frequency, for the jth test. The parameter vector p can be expressed as

$$p = p_0 + \delta p_v + \delta p_e, \tag{4}$$

where p_0 is the nominal parameter vector, δp_v is the change due to changes in the controlled conditions, and δp_e is the change due to other random factors. In this paper, a SVD technique [4] is used to generate an optimal linear interval model, which represents and covers all the identified parameter vectors p_j, as

$$H = \left\{ p | p = p_0 + \sum_{j=1}^{k} \alpha_j q_j, \quad \alpha_j \in \left[\alpha_j^-, \alpha_j^+ \right] \right\}, \tag{5}$$

where α_j is the jth identified uncertainty parameter corresponding to the basis vector q_j. The uncertainty parameter bounds are normalized to the first interval length, where the first interval length is 1. The interval lengths, which are in descending order, indicate the distribution of the parameter variation in the direction of the identified parameter vectors q_j.

3. Description of testbed

Fig. 1 shows a photograph of the assembled test-bed suspended configuration. A spring/cabin suspension system is designed to have the frequencies of suspension modes below the first structural flexible mode. As shown, the torus-segmented construction has twelve 0.181-m diameter tubes arranged to form a circle. Tubes are fabricated using a proprietary thermoplastic graphite epoxy composite. When this material is heated above

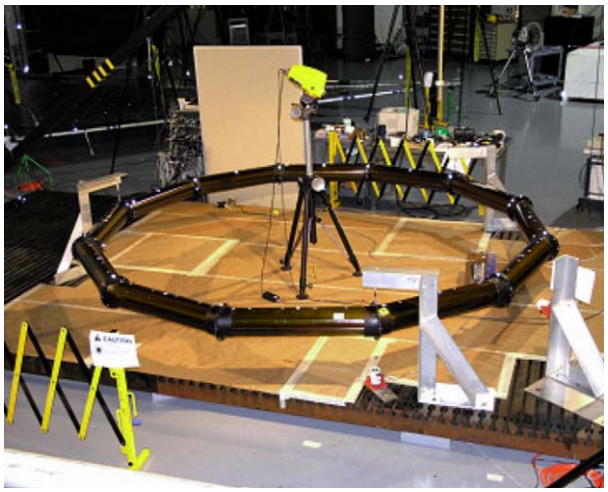

Fig. 1. Torus structure for testing.

its glass-transition temperature, the stiffness decreases enough to allow it to be folded or rolled, and thus packaged into a small volume. Rigid joints connecting the sections of the torus are cast from glass filled urethane. A joint is glued at each end of the tubes to form a torus tube/joint assembly. The torus/joint assemblies are fasten with bolts to form the torus. The structure was rigidized prior to its assembly.

For dynamic testing, an electromagnetic shaker, Ling Dynamic Systems V203, is connected to the torus perpendicular to the membrane plane. Forces are imparted to the torus at a hard point on the polyurethane collar. A thread mounted PCB 208 force gage is used to measure input excitation force at shaker drive points and a Nylon stinger (3/32″ diameter) is used to connect the shaker to the structure. Velocity response was measured with an Ometron VH300+ laser Doppler vibrometer (LDV). FRF data was collected using the shaker input force as reference.

4. Experimental results

To investigate the dynamic characteristics of the torus structure, experiments are conducted using sine-sweep excitation to compute the FRF. To improve the accuracy of the identified parameters for each mode [4], blocks of FRF data are collected with the sine-sweep frequency range restricted to a narrow frequency range. Fig. 2 shows the FRF data for the first two structural modes between 14 and 15 Hz for four cases under various test conditions, where the measured conditions are temperature and input force. Here the measured temperature is in Fahrenheit; the input force is the root-mean-square (rms) of the sine-sweep excitation and its unit is Newton. The natural frequency of the first structural mode is near 14.3 Hz, and there are two closely spaced modes between 14 and 15 Hz as shown in Fig. 2. Fig. 3 shows the FRF data for the third mode around 38 Hz for four cases. During testing it was observed that the natural frequencies of these three modes decrease as temperature and/or input force increase. To study the parameter uncertainty, various tests under different conditions are conducted. Fig. 4 shows the identified natural frequencies and damping ratios of the third mode for 27 tests with a rectangular envelope superimpose indicating the identified interval model. Data points plotted with '*' are the results of five tests with the same temperature 69.6°F and the input force increasing from 0.54 to 3.21 N. Data points plotted with '○' are the results of eight tests with temperatures ranging from 76.3°F to 76.1°F, and the input force increasing from 0.54 to 3.21 N. Four tests conducted with the same input force show no appreciable change in the identified parameters. Data points plotted with '·' are the results of 14 tests with both temperature changes, ranging from 80.1 to 80.9°F, and input force changes, ranging from 0.54 to 3.21 N. There are four tests with the same input force 0.54 N and small temperature increase resulting in a small reduction of the natural frequency. There are five pairs of identified parameters, where each pair with closed identified parameters corresponds to two tests with the same input force. The envelope in Fig. 4 corresponds to the identified interval model generated from the identified parameters of these 27 tests. This

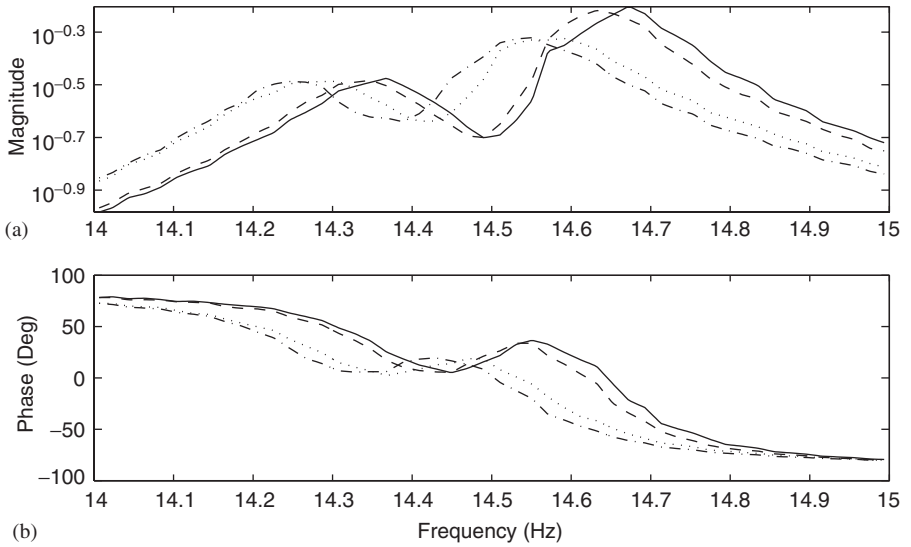

Fig. 2. FRF data between 14 and 15 Hz under various test conditions: (a) magnitude, (b) phase: — (69.5°F, 0.54 N); - - - (69.5°F, 1.61 N); ··· (79.1°F, 0.54N); - · - (78.3°F, 1.61 N).

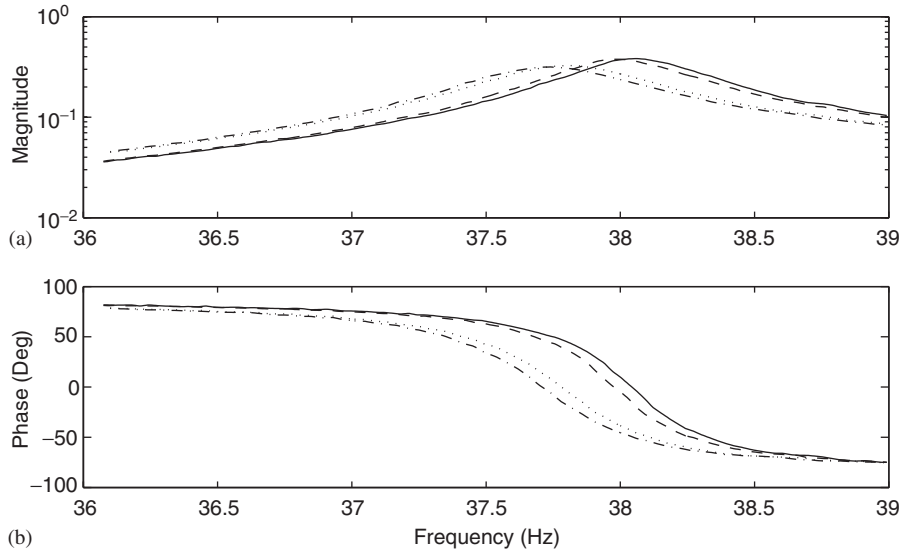

Fig. 3. FRF data between 36 and 39 Hz under various test conditions: (a) magnitude, (b) phase: — (69.6°F, 0.54 N); - - - (69.6°F, 1.61 N); ··· (80.3°F, 0.54 N); - · - (80.8°F, 1.61 N).

identified interval model of damping ratio and natural frequency (Hz) is

$$P = \begin{bmatrix} 0.00629 \\ 38.062 \end{bmatrix} + \alpha_1 \underbrace{\begin{bmatrix} 0.00195 \\ -0.383 \end{bmatrix}}_{q_1} + \alpha_2 \underbrace{\begin{bmatrix} 0.00220 \\ 0.340 \end{bmatrix}}_{q_2}, \quad \alpha_1 \in \begin{bmatrix} 0 & 1 \end{bmatrix}, \quad \alpha_2 \in \begin{bmatrix} -0.0605 & 0.0302 \end{bmatrix}.$$

The second interval length, 0.0907 (0.0302 + 0.0605), is 9.07% of the first interval length (= 1), consequently, the frequency and damping uncertainty of the third mode is dominated by α_1. As expected, the envelope computed using the interval model parameters precisely covers all the identified models and the directions associated with the edge lines of the rectangular envelop are given by the basis vectors q_1 and q_2.

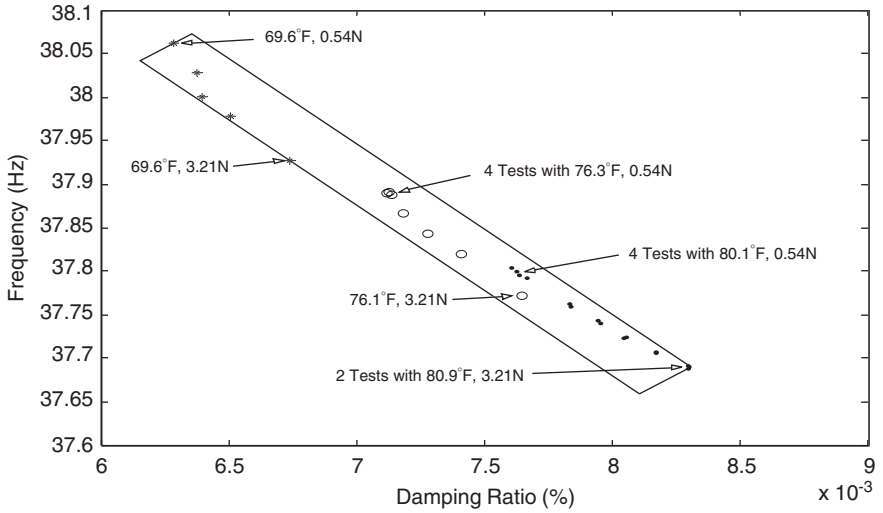

Fig. 4. Identified parameters of the 3rd mode under various test conditions: * (69.6°F, 0.54–3.21 N); ○ (76.3–76.1°F, 0.54–3.21 N); ⋯ (80.1–80.9°F, 0.54–3.21 N).

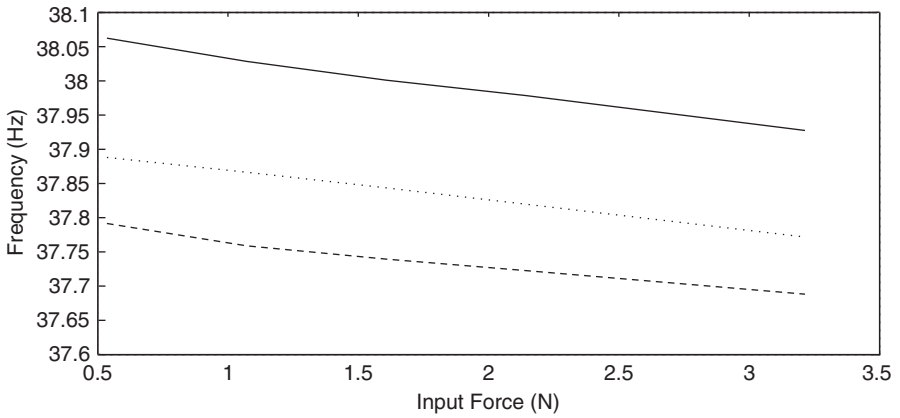

Fig. 5. Identified natural frequency of the 3rd mode for various input force: — (69.6°F); ⋯ (76.3–76.1°F); - - - (80.1–80.9°F).

The direction of the parameter change due to temperature change is close to the direction of the first basis vector q_1, and the direction of the parameter change due to input force variation is also close to that of q_1. The parameter change due to temperature variation is more significant than the change due to input force variation. Fig. 5 shows the natural frequency as a function of input force for the three groups in Fig. 4. All three lines are close to straight lines parallel to each other, indicting that the natural frequency of the 3rd mode decreases linearly as the input force increases.

In general, the identified damping ratios are more sensitive to noise than the identified natural frequencies. Since the damping ratios of the first two modes do not change much with input gain, changes in damping ratio are attributed to other random factors. For this reason, the interval modeling technique is only applied to the identified natural frequencies of the first two modes resulting in the following interval model:

$$P = \begin{bmatrix} 14.366 \\ 14.667 \end{bmatrix} + \alpha_1 \underbrace{\begin{bmatrix} -0.122 \\ -0.170 \end{bmatrix}}_{q_1} + \alpha_2 \underbrace{\begin{bmatrix} 0.119 \\ -0.173 \end{bmatrix}}_{q_2}, \quad \alpha_1 \in \begin{bmatrix} 0 & 1 \end{bmatrix}, \quad \alpha_2 \in \begin{bmatrix} -0.0454 & 0.0292 \end{bmatrix}.$$

In this case, the second interval length is 7.46% of the first interval length and therefore the parameter uncertainty is dominated by the direction q_1. Fig. 6 shows the variation in the identified natural frequencies of the first two modes from 15 tests with a rectangular envelope corresponding to the identified interval model. Data points plotted with '*' are the results of 5 tests with the same temperature 69.5°F and the input force increasing from 0.54 to 2.68 N. Data points 'o' are the results of 10 tests with the temperature decreasing from 78.8°F to 77.7°F, and the input force increasing from 0.54 to 2.68 N. There are five pairs of identified parameters, where each pair corresponds to two tests with same input force. The identified natural frequencies of each of three middle pairs show some changes due to temperature change. The direction of parameter change due to temperature or input force variation is close to the direction of the first basis vector q_1. The parameter change due to temperature variation is more significant. Fig. 7 shows the natural frequencies as a

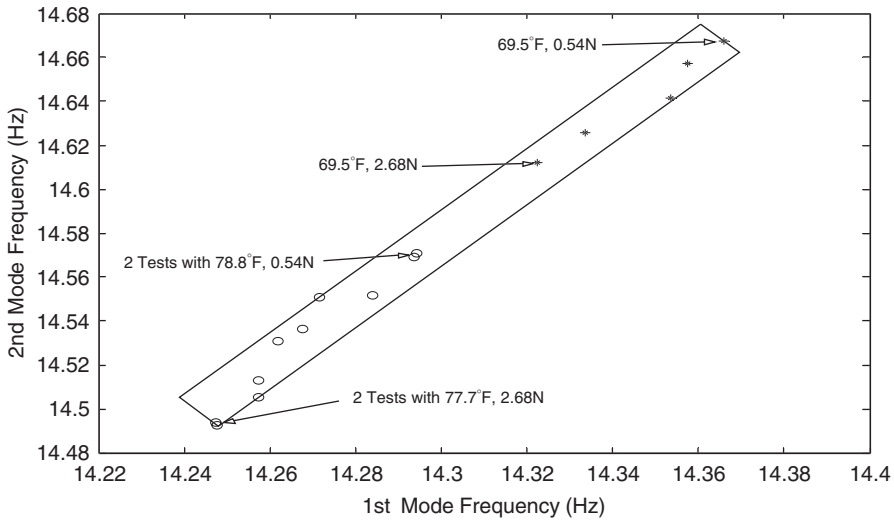

Fig. 6. Identified natural frequencies of the first two modes under various conditions: * (69.5°F, 0.54–2.68 N); ○ (78.8–77.7°F, 0.54–2.68 N).

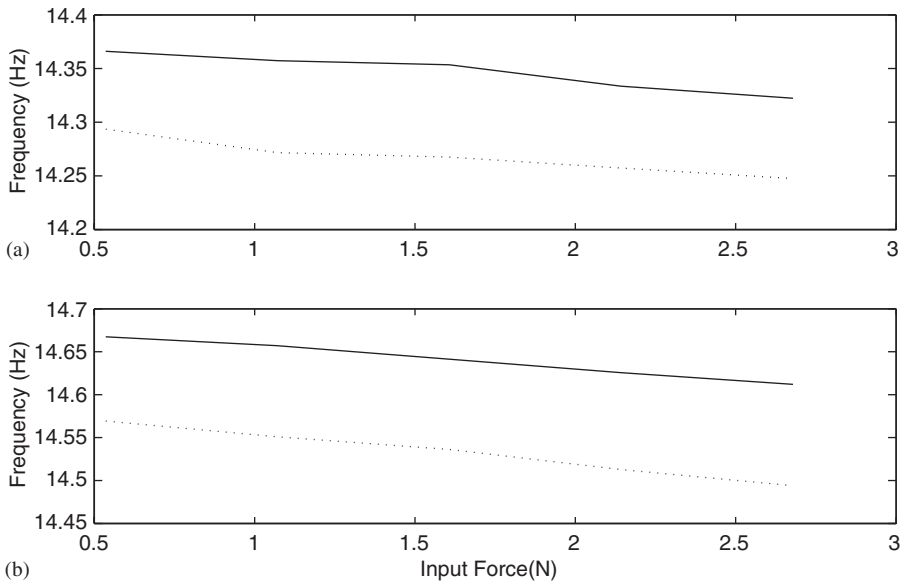

Fig. 7. Identified natural frequencies of the first two modes for various input force: (a) 1st mode, (b) 2nd mode: — (69.6°F); ··· (78.8–77.7°F).

function of input force for the two groups in Fig. 6. Both lines in each figure are close to straight lines parallel to one another, indicating that the natural frequencies of the first two modes decrease linearly as input force increases.

Only six structural modes are identified within 100 Hz.Table 1 lists the identified parameters at 69.6°F with low input force of sine-sweep excitation. As observed with modes 1–3 the natural frequencies of modes 4–6 also decrease as temperature or input force increases. One potential explanation is that the tube stiffness decreases as temperature increases. Table 2 shows the natural frequencies of the finite element model below 100 Hz of the nominal system, and the system with 1% reduction of all the modulus, tube modulus, tube shear modulus, and joint modulus. There are 15 structural modes below 100 Hz. The loss of 1% modulus results in 0.5% reduction of all the natural frequencies except the first two modes and the mode with frequency 38.36 Hz. For a single-degree-of-freedom system, a reduction of 1% stiffness results in 0.501% ($= [1 - \sqrt{0.99}] \times 100\%$) decrease of natural frequency, which is close to 0.5%.

All the experiments are conducted with the ambient temperature between 69.5°F and 83.0°F. When the tests are conducted at 69.5°F, the temperature fluctuates from 69.5°F to 69.6°F, and the tests for all the modes could be conducted under various input force at this temperature T_0, which is used as the low temperature for comparison. The highest temperature for the tests of each mode is about 10°F higher than T_0.

The range of effective excitation force varies for each frequency band. For the first two modes, the results with the force between 0.54 and 2.68 N are shown in Fig. 4. The FRF data for the first two modes is noisy when the input force is lower than 0.54 N and significant vibration of resonance appears when the input

Table 1
Identified parameters at 69.6°F

Mode	Frequency (Hz)	Damping (%)
1	14.37	0.47
2	14.67	0.53
3	38.06	0.63
4	67.66	0.76
5	92.26	0.60
6	93.54	0.96

Table 2
Natural frequency changes of finite element model due to modulus change

Nominal system frequency (Hz)	1% Modulus loss frequency (Hz)	Frequency decrease (%)
13.76	13.71	0.43
13.78	13.72	0.43
20.72	20.62	0.50
20.72	20.62	0.50
37.77	37.58	0.50
38.36	38.18	0.49
52.58	52.31	0.50
52.59	52.32	0.50
66.73	66.39	0.50
66.73	66.40	0.50
86.66	86.23	0.50
86.66	86.23	0.50
89.98	89.53	0.50
89.98	89.53	0.50
99.11	98.62	0.50

Table 3
Natural frequency changes due to temperature and input force changes

Mode	Frequency decrease for 10°F temperature increase (%)	Frequency decrease for 1 N force increase (%)	Frequency decrease for 1% modulus decrease (%)
1	0.663 (1.55% modulus)	0.142	0.428
2	0.734 (1.72% modulus)	0.176	0.427
3	0.694 (1.39% modulus)	0.132	0.500
4	0.786 (1.57% modulus)	0.132	0.500
5	0.691 (1.38% modulus)	0.119	0.500
6	0.780 (1.56% modulus)	0.099	0.500

frequency is higher than 2.68 Hz. The effective input force range for modes 4–6 is about between 0.8 and 5 N. Table 3 lists the results of the reduction of nature frequencies due to the increase of temperature and input force. In Table 3, the reduction of natural frequencies, due to the loss of 1% modulus, for modes 3–6 is chosen as 0.5% since the reduction of natural frequencies except the first two modes in Table 2 is close to 0.5%. When the temperature increases 10°F, the reduction of the natural frequency of each mode is about the change due to 1.5% modulus decrease. When the input force of sine-sweep excitation for each mode increases from the minimum to the maximum, the reduction of the natural frequency for that mode is about that due to 1% modulus decrease. The parameter change due to temperature variation is more dominant.

5. Concluding remarks

This paper presents the uncertainty quantification of structural dynamics of a lightweight inflatable/rigidizable torus. To investigate and quantify changes in natural frequencies, blocks of FRF data are collected with the sine-sweep excitation restricted to specified narrow frequency ranges. The results show that the identified natural frequencies decrease significantly as temperature increases. The reduction of natural frequencies, due to a 10°F temperature increase, corresponds to a 1.5% modulus reduction of the whole structure. When plotted as a function of input level, the identified natural frequencies decreased, indicating a softening behavior of the structure. Observed reductions in natural frequencies due to changes in the maximum excitation force correspond to about 1% modulus reduction. Results from the computed interval models show that the parameter uncertainty in every case is dominated by the direction of the first basis vector associated with α_1. This indicates that the change due to temperature shares the same pattern as the change due to input force, and the uncertainty associated with all other unconsidered factors is relatively small. By using sine-sweeps in the narrow frequency bands high quality experimental data can be collected reducing the identified parameter uncertainty due to other random factors. The study shows that the uncertainty due to temperature changes is the most dominant.

References

[1] C.H.M. Jenkins (Ed.), *Gossamer Spacecraft: Membrane and Inflatable Structures Technology for Space Applications, Vol. 191, Progress in Astronautics and Aeronautics Series*, AIAA, Reston VA, 2001.

[2] A.B. Chmielewsk, Overview of Gossamer Structures, in: C.H.M. Jenkins (Ed.), *Gossamer Spacecraft: Membrane and Inflatable Structures Technology for Space Applications, Vol. 191, Progress in Astronautics and Aeronautics Series*, AIAA, Reston VA, 2001, pp. 1–20.

[3] O. Adetona, L.H. Keel, L.G. Horta, D.P. Cadogan, G.H. Sapna, S.E. Scarborough, Description of new inflatable/rigidizable hexapod structure testbed for shape and vibration control, AIAA-2002-1451, in: *Proceedings of the 43rd AIAA Structures, Structural Dynamics and Materials Conference*, Denver, Co, April 22–25, 2002.

[4] J.-S. Lew, L.G. Horta, Parametric uncertainty quantification of an inflatable/rigidizable hexapod, in: *Proceedings of the AIAA Fifth Gossamer Spacecraft Forum, Palm Springs*, CA, 2004.

[5] D.J. Ewins, *Modal Testing: Theory, Practice, and Applications*, second ed., Research Studies Press Ltd., Baldock, Hertfordshire, England, 2000.

[6] B.H. Thacker, The Role of Nondeterminism in Computational Model Verification and Validation, in: *Proceedings of the 46th AIAA Structures, Structural Dynamics and Materials Conference*, Austin, TX, April 18–21, 2005.
[7] A.C. Rutherford, J.E. Hylok, R.D. Maupin, M.C. Anderson, Practical Application of Uncertainty-Based Validation Assessment, in: *Proceedings of the 46th AIAA Structures, Structural Dynamics and Materials Conference*, Austin, TX, April 18–21, 2005.
[8] T. Kailath, *Linear Systems*, Prentice-Hall, Englewood Cliffs, NJ, 1980.